

An atomic-level perspective of shear band formation and interaction in monolithic metallic glasses

D. Şopu^{a,b,*}, F. Moitzi^a, N. Mousseau^c, J. Eckert^{a,d}

^aErich Schmid Institute of Materials Science, Austrian Academy of Sciences, Jahnstraße 12, Leoben A-8700, Austria

^bFachgebiet Materialmodellierung, Institut für Materialwissenschaft, TU Darmstadt, Otto-Berndt-Straße 3, Darmstadt D-64287, Germany

^cDépartement de Physique and Regroupement Québécois sur les Matériaux de Pointe, Université de Montréal, Canada

^dDepartment of Materials Science, Chair of Materials Physics, Mountainuniversität Leoben, Jahnstraße 12, Leoben A-8700, Austria

ARTICLE INFO

Article history:

Received 23 July 2020

Revised 2 September 2020

Accepted 8 September 2020

Keywords:

Metallic glasses

shear bands

molecular dynamics simulations

plasticity

shear transformation zones

heterogeneities

ABSTRACT

Understanding the relationship between nanoscale structural heterogeneities or elastic fluctuations and strain localization in monolithic metallic glasses remains a long-standing underlying issue. Here, an atomic-level investigation of the correlation between elastic and structural heterogeneities and the mechanisms of shear banding in CuZr metallic glass is conducted using molecular dynamics simulations. The shear band formation and propagation processes and the intersection mechanism of multiple shear bands are evaluated by means of local entropy-based structural identification and von Mises stress calculation. The shear band follows the path of lower order and high entropy while shear deflection and branching occur when approaching regions of low entropy. The local von Mises stress calculation allows predictions on the shear band direction and the propensity for activation and propagation prior to yielding and sheds light on shear band branching and multiplication processes.

© 2020 Elsevier Ltd. All rights reserved.

1. Introduction

Enhanced plasticity in metallic glasses (MGs) is ascribed to the formation of many shear bands with small shear offsets [1]. This can be achieved in composite MGs where crystalline heterogeneities promote shear band nucleation and multiplication [2–5]. Furthermore, the interaction with crystalline inclusions blocks the propagation of shear bands and imposes a confinement on the shear offsets [6,7]. A high density of shear bands, and consequently large plastic strain, can also be achieved in monolithic MGs with higher Poisson's ratio [8,9]. Although they have no microstructure, here atomic-scale structural heterogeneities and elastic fluctuations control the strain distribution and the processes of shear band formation, propagation and multiplication [10–13]. The evolution and intersection of a large population of shear bands blocks their propagation and stimulates the initiation of even more shear bands, delaying in this way the onset of catastrophic failure [14]. Moreover, the interaction of shear bands changes their dynamics and morphologies, increases the yield stress and promotes work-hardening during deformation [15–18]. Although shear band interactions have been widely used to explain an increased strain to failure and

deformation-induced hardening in MGs [15], the major challenge is to understand and control the shear band blocking mechanism.

While over the last decades substantial progress has been made in post-mortem investigations of the structure of shear bands only few analyses of the shear band dynamics have been reported owing to the spatial and temporal scales of the deformation processes [19,20]. To date, few methods have been proposed to investigate shear band dynamics and blocking mechanisms [16,17,19,21–23]. Nanoindentation [17], atomic force microscopy [22,23] and high-resolution transmission electron microscopy [16] studies have provided a consistent picture of shear band dynamics but could not explain the complex and mutual interaction process and what happens at the shear band intersection points as understanding what drives the changes in strain localization behavior related to the phenomena of shear band propagation and intersection requires systematic atomic-level investigations.

Computer simulations provided insight into the atomic-scale structure and deformation processes in MGs [5,11,24–26]. An important goal of atomistic modeling was to define environmental descriptors to identify and characterize the atomic scale heterogeneities and provide a detailed structure-property relationship for metallic glasses [27,28]. Here, we derive a local fingerprint based on an approximate expression for the entropy using atomistic simulations, highlighting the strength of the correlation between structural heterogeneities and strain localization in mono-

* Corresponding author.

E-mail address: daniel.sopu@oeaw.ac.at (D. Şopu).

lithic glasses. The local entropy shows a high predictive power and allows for gradual representation of the local structure without any prior information on a reference configuration. Special emphasis is also given to the von Mises stress that allows us to characterize elastic fluctuations and predict the spatial and temporal evolution of the atomic strain prior shear band propagation and particularly at the shear band intersection point.

2. Materials and methods

To overcome experimental technical difficulties associated with the observation of the fast processes of shear band propagation and interaction large-scale molecular dynamics (MD) simulations were carried out using the LAMMPS software [29]. The $\text{Cu}_{64}\text{Zr}_{36}$ metallic glass has been simulated using the interatomic potential developed by Mendeleev et al. [30]. The starting liquid structure was created by randomly distributing 968,000 atoms in a box of $111.0 \times 55.5 \times 2.5 \text{ nm}$ with periodic boundary conditions. Uniform-acceptance force bias Monte Carlo [31] and MD in a NPT ensemble were used alternately, in order to deal with the overlap between the atoms during the initial equilibration of the liquid structure. The liquid structure was cooled to 50 K above T_g ($\approx 800 \text{ K}$) at a rate of 10 K/ps starting from 1600 K. Since the local structure of metallic glasses mostly develops in a temperature range of 100 K around T_g [26] the cooling rate was reduced to just 0.01 K/ps at that temperature. After cooling down to 50 K below T_g an annealing for 4.0 ns was performed. The final cooling to 50 K was then done with 10 K/ps . The cooled sample was replicated twice along the z-direction and notched in order to get a tensile sample with a preferred site for shearing. Open boundaries in y-direction and periodic boundaries in the x- and z-directions were applied. Tensile simulations were performed under constant engineering strain rate of $4 \times 10^7 \text{ 1/s}$ in a NPT ensemble at 50 K. The local structure was analyzed in terms of Voronoi polyhedra obtained from Voronoi tessellation. The calculation and visualization of von Mises strains and von Mises stresses were carried out with OVITO using the python scripting interface [32]. These two quantities were evaluated at each atomic site relative to its neighbors within a cutoff including the third nearest neighbor shell.

The Activation-Relaxation Technique (ART nouveau or ARTn) [33–35] was also used to sample the energy landscape and quantify activation pathways between adjacent minima energetically [36]. A $\text{Cu}_{64}\text{Zr}_{36}$ glassy structure with 8000 atoms were created following the above mentioned procedure. The system was then relaxed to zero kinetic energy with global interatomic forces minimized to 10^{-6} eV/\AA . A number of 10 relaxation pathways were searched for each atom starting from the same initial structure. Additionally, a novel local entropy-based structural identification method was used to investigate the influence of structural heterogeneity on shear band evolution (see Supplementary Materials)[37].

3. Results

3.1. Influence of structural heterogeneity on shear band dynamics

Although the structural disorder of MGs entails the absence of structural features such as grain and phase boundaries, dislocations and stacking faults, they possess a high degree of short-range order (SRO) and even medium-range order (MRO) [38,39]. The most commonly found SRO clusters in MGs have a preference to develop five-fold symmetry. These locally favored structure motifs are accompanied by more unfavorable polyhedra, which are needed to fill the spaces between the more ordered clusters and to connect the backbone structure. These spacing structures are commonly termed as Geometrical Unfavorable Motifs (GUMs) [11], anti-site

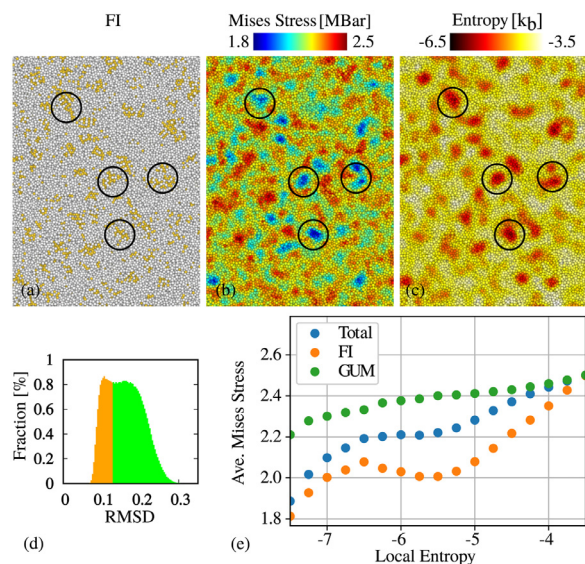


Fig. 1. Structure analysis in a macroscopically relaxed $\text{Cu}_{64}\text{Zr}_{36}$ metallic glass. (a): FI clusters (yellow atoms) are displayed with a RMSD smaller than 0.13 and are obtained from polyhedral template matching compared to an ideal reference configuration. (b): Local high densities of FI clusters (black circles) show lower von Mises stress and therefore lower distortion energy. (c): Entropy-based fingerprint showing that ordered regions of FI clusters have low entropy and high structural order. In the lower panel the relationship between local stress and entropy is presented. (d): Histogram of the RMSD for all icosahedral polyhedra from Voronoi tessellation. The orange area of the histogram refers to only slightly distorted polyhedra with starting chemical ordering. These polyhedra were depicted in (A). The green part of the histogram represents strongly distorted icosahedral polyhedra. (e) Von Mises stress vs local entropy graphs for the total number of atoms (blue points), closed packed FI clusters (orange points) and GUMs (green points). (For interpretation of the references to colour in this figure legend, the reader is referred to the web version of this article.)

point defects [40], unfavorable clusters [41] or liquid-like regions [42]. These disordered regions are more susceptible to reconfiguration via thermal- or stress-induced rearrangement and can be seen as soft spots in metallic glasses [42,43]. The local atomic structure is of key importance in determining the energy barrier and the propensity for shear transformation zones (STZs) activation and percolation and ultimately, controls the deformation behavior of MGs [44].

Even though the sample is macroscopically relaxed, down to the atomic level, MGs show heterogeneous structures. The full icosahedra (FI) in Fig. 1a are displayed with a root mean squared deviation (RMSD) smaller than 0.13 (Fig 1d), which corresponds to a low distortion compared to an ideal reference icosahedron. The von Mises stress in the FI close-packed clusters is significantly lower compared to the surrounding (see Fig. 1b) and, in general, local stress fluctuations correlate with the local structure. The von Mises stress corresponds to the deformation energy due to pure distortion. The more ordered regions are in an energetically favorable state and are shielded from the influence of stress and deformation. Packing frustration explains higher von Mises stresses in regions of GUMs, where the atoms are forced in unfavorable positions. It should be noted that the level of distortion for the FI clusters was calculated based on a reference configuration; the choice of RMSD cutoff was based on the occurrence of a distinctive peak in the RMSD. The quantification is, therefore, only possible if a priori information about the polyhedra is available and, hence, the level of disorder in liquid-like regions (disordered regions) remains elusive.

The local entropy provides a possibility for gradual representation of disorder without the previously discussed limitations. Based on the Piaggi model [37], the local entropy calculation involves only a local approximation of the radial distribution function and

does not require any information on the geometry of SRO clusters. The local entropy calculation includes both, the vibrational and the configurational contributions. However, since our simulations are done at a very low temperature of 50 K the vibrational entropy has a limited contribution. In the case of $\text{Cu}_{64}\text{Zr}_{36}$ metallic glass areas of low local entropy correspond to FI clusters, while the liquid-like clusters (non-icosahedral) have high entropy (see Fig. 1c). Additional information about the entropy distribution of FI clusters and GUMs is provided in the Supplementary Materials. Thus, the local entropy function solely quantifies the level of ordering and, consequently, can be used as a fingerprint to track the influence of structural heterogeneity on shear band dynamics. Under loading, the soft spots, characterized by high entropy, would show a high propensity for STZ activation. Following, a shear band forms by the coalescence of an alignment of STZs along a specific direction. Moreover, local entropy and von Mises stress are mutually dependent: both increase with decreasing degree of order (Fig. 1e). However, the two descriptors are not perfectly connected and in the low entropy range, the Mises stress increases drastically followed by a decrease. Entropy is a measure of disorder of the glassy structure but is not sensitive to small elastic distortions of FI clusters. On the other hand, the von Mises stress quantifies the force required to distort the material locally and change the shape of the cluster leaving its volume unchanged. Thus, FI clusters, with a well-defined shape and low entropy, are very sensitive to angular distortions resulting in strong fluctuations of the Mises stress (orange line in Fig. 1e). Nevertheless, a low degree of order in GUMs makes them insensitive to distortion, resulting in a small variation of von Mises stress with entropy (green line in Fig. 1e). Additionally, an investigation of the correlation between the local entropy and the atomic volume distributions can be found in Supplementary Materials.

The large variations in the atomic-scale order and elastic fluctuations confirm that MGs are highly heterogeneous structures. Hence, even in a monolithic MG the activation of STZs and their percolation can be perturbed by local fluctuations. Under external stress, one can expect strong variation in the strain localization and, therefore, changes in the atomic-level mechanism of shear banding. By analyzing in comparison the evolution of the local entropy and shear strain, while still being in the elastic regime (defined here as time frame $\Delta t=0$ ps), two notable features can be observed. First, macroscopic strain is only accommodated in areas with high entropy and changes in the atomic strain can be only seen there (see Fig. 2). Second, the low entropy regions corresponding to closed-packed clusters remain undeformed and undergo a collective rigid body motion during deformation. The occurrence of discrete deformation processes is correlated with the observed variation in the atomic strain in the GUM regions even before the yield point. The localized elastic deformation of the material can be explained by the spatial fluctuations of local elastic properties. It is known that the elasticity strongly depends on the local atomic order [45]. The shear modulus and, therefore, the resistance against shear deformation is more affected than the bulk modulus. Thus, the strain response to an external loading will be first accommodated in softer (disordered) regions mostly through local elastic shear relaxations [26].

At some point ($\Delta t=160$ ps) plastic deformation will set in after further straining the sample. The deformation of the sample is now strongly localized and a shear band nucleates at the notch, which acts as a stress concentrator (see Fig. 2). When analyzing the local entropy one can see that the shear band tries to follow the path of lower order. This can easily be explained by recalling the already known correlation between the propensity of STZ activation and structural order. The activation of STZs is significantly easier in disordered and highly strained regions. We reinforce this argument by calculating with ARTn the activation energies for 20% of atoms

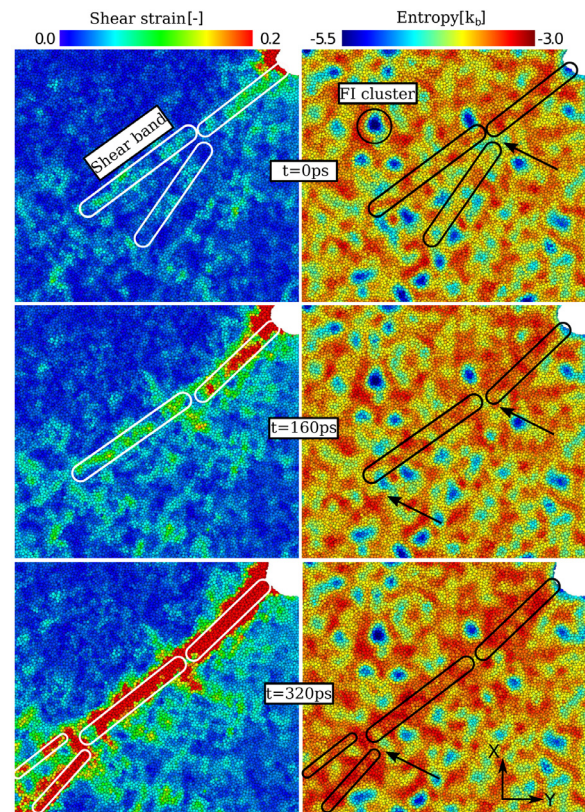


Fig. 2. The evolution of shear strain and local entropy during deformation and shear band formation in a monolithic $\text{Cu}_{64}\text{Zr}_{36}$ metallic glass. The shear band follows the region of high entropy. It deflects and branches when it interacts with regions of lower entropy.

with the lowest and the highest entropy. The histograms of the activation barriers correlate with the local structure in MG [46,47]. As can be seen in Fig. 3 the atoms of low entropy experience a higher average activation energy barrier of about 2.2 eV compared to those atoms of high entropy (≈ 1.7 eV). Furthermore, the atoms of high entropy show a higher population of events of low energy corresponding to fast atomic relaxations or γ -relaxation at energies below 0.3 eV [48]. Thus, the fast relaxation mechanism could be correlated to the local distortion of elastic heterogeneities within the elastic regime.

At the time frame $\Delta t=320$ ps, the shear band tip, however, approaches the higher ordered regions of low entropy and then deflection and branching occur (Fig. 2). We recently showed that a shear band in MG can be seen as an alternating sequence of STZs behaving as Eshelby inclusions and vortex-like (rotating) structures [5,49]. Here, the rotational displacement of the atoms around the STZ does not exceed the activation threshold for another STZ in the harder ordered region [5,26]. However, the local stresses reach the activation threshold for STZs in the softer and more disordered vicinity. The percolation path of the STZ-vortex sequence will therefore be disturbed by the ordered regions acting as local barrier for the percolating shear band. Nevertheless, the ordered regions are not completely unaffected by the shearing process. They get consumed by the slipping shear band due to the heat generation in the band during its operation [50].

3.2. Dynamic interaction between shear bands

In a ductile monolithic glass, besides the interaction with atomic-scale structural heterogeneities, shear bands interact with each other. To capture the atomistic mechanisms of the shear

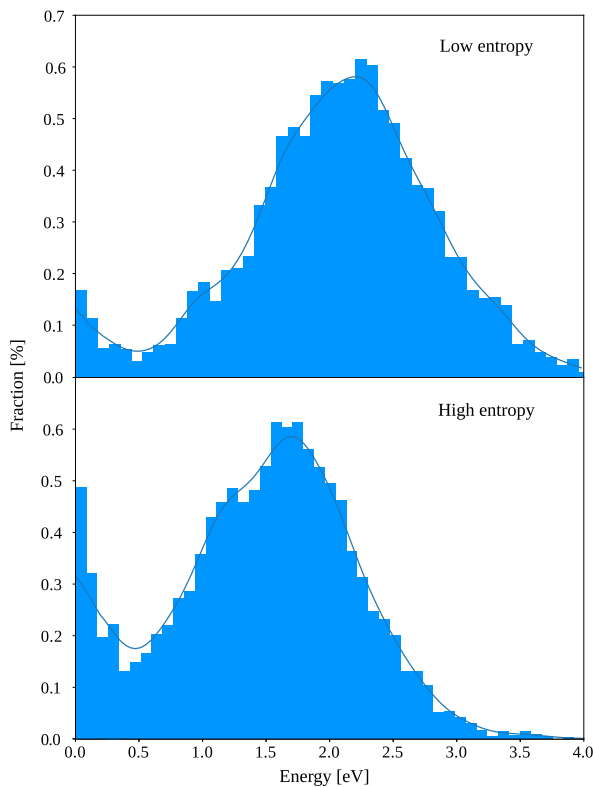


Fig. 3. Histograms of activation energies from a saddle point search of the potential energy landscape for 20% of atoms of low (upper panel) and high (lower panel) entropy. Atoms of low entropy experience higher average activation energy barriers compared to those atoms of high entropy.

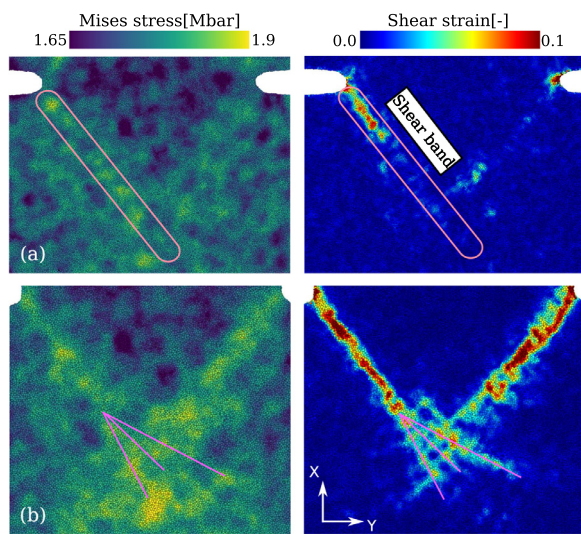


Fig. 4. The evolution of von Mises stress (left hand side panels) and von Mises strain (right hand side panels) in a $\text{Cu}_{64}\text{Zr}_{36}$ sample with two notches deformed in tension. (a) The stress distribution predicts the propensity for activation and propagation of the shear bands prior strain localization. (b) When the two shear band intersect the stress overlapping at the intersection point modifies the stress state, causing shear band branching and multiplication.

band interaction, a $\text{Cu}_{64}\text{Zr}_{36}$ sample with two notches was prepared. At the yield point a shear band initiates from one notch and starts propagating along a preferential direction while at the second notch no shear band is present (see Fig. 4a). More interesting is the distribution of the von Mises stress that closely correlates with the shear band path. The von Mises stress shows a

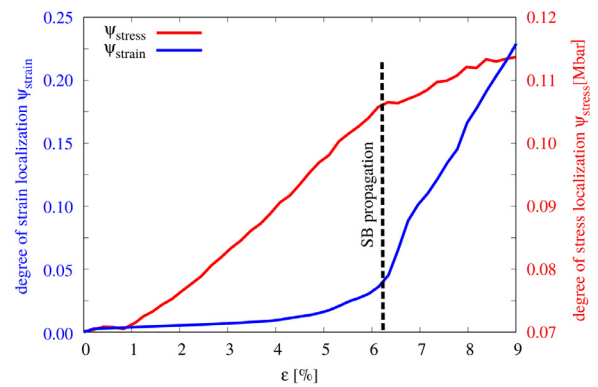


Fig. 5. The degree of strain and stress localization parameters, ψ_{strain} and ψ_{stress} , in a $\text{Cu}_{64}\text{Zr}_{36}$ sample with two notches deformed in tension. The ψ_{stress} never starts from zero value because local stress fluctuations can be seen even in the relaxed (undeformed) MG.

heterogeneous distribution that clearly precedes the shear band path and leads to the evolution of the shear band in a certain direction. As expected from theory, the shear band follows well-defined areas of high distortional stress exceeding the activation stress for plastic deformation. The local stress state also determines from which notch the shear band propagates first. The left shear band is further developed due to the higher local Mises stress in extension of the left notch in Fig. 4a. At the beginning, the von Mises stress, which has distinct maxima at about 45° and 135° inclined to the notches, is imposed by the sample geometry. The shearing at notches intensifies the von Mises stress pattern. The von Mises stress increases in regions that lay on the extension on the propagating shear band. Hence, the shear bands interact through elastic heterogeneities long before the plastic zones of the two shear fronts start to intersect. The complex distribution of the von Mises stress on the prospective intersection point of the shear bands leads to shear band branching (Fig. 4b). The overlapping of the stress fields of the two shear fronts drastically increases the local von Mises stress and affects its distribution. This, ultimately, perturbs the STZ percolation process and the shear band dynamics. The propagation directions of the STZs align with the complex stress states at the intersection point resulting in the formation of three new shear bands with different specific directions. Following the shear branching process and further shearing along this direction, the von Mises stress in the primary shear band decreases. However, the level of stress in the right shear band remains high while its further propagation is blocked by the other shear band. As a result, the von Mises stress, which corresponds to the local distortion energy, can a priori predict the shear band direction and the propensity for activation and propagation.

A quantitative evaluation of the aforementioned correlation between the local stress distribution and strain localization or how elastic and plastic fluctuations evolve under loading is performed based on strain and stress localization parameters (Fig. 5).

$$\psi_{strain/stress} = \sqrt{\frac{1}{N} \sum_{i=1}^N (\eta_i^{Mises} - \eta_{ave}^{Mises})^2}$$
, where η_{ave}^{Mises} is the average von Mises strain/stress over all atoms in the simulation cell [45]. Large values of these two parameters indicates large variation in the von Mises stress and strain during the deformation process and hence, an increased heterogeneity. As expected, ψ_{stress} starts to increase early in the elastic regime while ψ_{strain} displays strong variations only in the stage of the plastic deformation when a shear band initiates (see Fig. 5). The local elastic heterogeneity (regions of GUMs) starts to activate at stresses well below the macroscopic yield while structural heterogeneities emerge only lately as precursors to shear banding. Moreover, once strain localization commences, the increase in ψ_{stress} gets weaker and cor-

relates to the decrease of the Mises stress along the shear front (Fig. 4). These observations help to explain why the spatial distribution of elastic fluctuations is responsible for the highly localized deformation process in MGs. During loading, the elastic heterogeneities along the maximum shear stress direction suffer continuously from elastic distortion exceeding at the yield point the activation stress for plastic deformation. As a result, a transition from elastic to plastic heterogeneities occurs which translates to STZ activation. Otherwise, a ductile MG with a low density of closed-packed clusters has a lower degree of elastic heterogeneity and hence, low probability for local stress accumulation leading to a more homogeneous strain distribution in the MG.

4. Conclusions

In summary, the correlation between elastic and structural heterogeneities and the atomic-level mechanisms of strain localization in monolithic metallic glasses was investigated. By using a novel local entropy-based structural identification method we found that the shear band follows the path of lower order and high entropy. Moreover, when the shear band approaches higher ordered regions of low entropy, shear deflection and branching occur promoting shear band multiplication. While the local entropy parameter shows an excellent ability to describe the complex spatio-temporal strain distribution process, the evolution of elastic fluctuations identified by von Mises stress calculation allows predictions on the shear band direction and the propensity for activation and propagation prior to yielding. The von Mises stress precedes the shear band path and leads to the evolution of the shear band at a certain place and direction. The intersection of multiple shear bands induces large stress fluctuations at the intersection point which, in turn, perturbs the STZ percolation process and, ultimately, leads to shear band branching and further multiplication.

Declaration of Competing Interest

The authors declare that they have no known competing financial interests or personal relationships that could have appeared to influence the work reported in this paper.

CRediT authorship contribution statement

D. Şopu: Conceptualization, Formal analysis, Supervision, Writing - original draft, Writing - review & editing. **F. Moitzi:** Data curation, Formal analysis, Writing - review & editing. **N. Mousseau:** Formal analysis, Writing - review & editing. **J. Eckert:** Supervision, Writing - review & editing.

Acknowledgments

D. Ş. acknowledges the financial support by the [Deutsche Forschungsgemeinschaft](#) (DFG) through Grant No. [SO 1518/1-1](#). Additional support was provided by the [European Research Council](#) under the ERC Advanced Grant INTELHYB (grant [ERC-2013-ADG-340025](#)). The authors are grateful for the computing time granted by the Lichtenberg high performance computer of Technische Universität Darmstadt and the high performance cluster of Montanuniversität Leoben. The authors acknowledge Dr. A. Stukowski for implementing the new local entropy parameter in OVITO software.

Supplementary material

Supplementary material associated with this article can be found, in the online version, at [10.1016/j.apmt.2020.100828](#)

References

- [1] A.L. Greer, Y.Q. Cheng, E. Ma, Shear bands in metallic glasses, *Mater. Sci. Eng.* 74 (4) (2013) 71–132.
- [2] D.C. Hofmann, J.Y. Suh, A. Wiest, G. Duan, M.L. Lind, M.D. Demetriou, W.L. Johnson, Designing metallic glass matrix composites with high toughness and tensile ductility, *Nature* 451 (7182) (2008) 1085–1089.
- [3] G. He, J. Eckert, W. Löser, L. Schultz, Novel ti-base nanostructure-dendrite composite with enhanced plasticity, *Nat. Mater.* 2 (1) (2003) 33–37.
- [4] D. Şopu, M. Stoica, J. Eckert, Deformation behavior of metallic glass composites reinforced with shape memory nanowires studied via molecular dynamics simulations, *Appl. Phys. Lett.* 106 (21) (2015), doi:10.1063/1.4921857.
- [5] D. Şopu, S. Scudino, X.L. Bian, C. Gammer, J. Eckert, Atomic-scale origin of shear band multiplication in heterogeneous metallic glasses, *Scr. Mater.* 178 (2020) 57–61.
- [6] M.W. Chen, A. Inoue, W. Zhang, T. Sakurai, Extraordinary plasticity of ductile bulk metallic glasses, *Phys. Rev. Lett.* 96 (2006) 245502, doi:10.1103/PhysRevLett.96.245502.
- [7] D. Şopu, K. Albe, J. Eckert, Metallic glass nanolaminates with shape memory alloys, *Acta Mater.* 159 (15) (2018) 344–351, doi:10.1016/j.actamat.2018.08.034.
- [8] W.H. Wang, J.J. Lewandowski, A.L. Greer, Understanding the glass-forming ability of Cu₅₀Zr₅₀ alloys in terms of a metastable eutectic, *J. Mater. Res.* 20 (9) (2005) 2307–2313.
- [9] G.N. Greaves, A.L. Greer, R.S. Lakes, T. Rouxel, Erratum: Poisson's ratio and modern materials, *Nat. Mater.* 10 (12) (2011). 986–986
- [10] F. Zhu, A. Hirata, P. Liu, S. Song, Y. Tian, J. Han, T. Fujita, M. Chen, Correlation between local structure order and spatial heterogeneity in a metallic glass, *Phys. Rev. Lett.* 119 (21) (2017) 215501.
- [11] E. Ma, Tuning order in disorder, *Nat Mater* 14 (6) (2015) 547–552.
- [12] D. Şopu, A. Foroughi, M. Stoica, J. Eckert, Brittle-to-ductile transition in metallic glass nanowires, *Nano Lett.* 16 (7) (2016) 4467–4471, doi:10.1021/acs.nanolett.6b01636.
- [13] C. Liu, R. Maaß, Elastic fluctuations and structural heterogeneities in metallic glasses, *Adv. Funct. Mater.* 28 (30) (2018) 1800388, doi:10.1002/adfm.201800388.
- [14] L.F. Liu, L.H. Dai, Y.L. Bai, B.C. Wei, J. Eckert, Behavior of multiple shear bands in zr-based bulk metallic glass, *Mater. Chem. Phys.* 93 (1) (2005) 174–177.
- [15] J. Das, M.B. Tang, K.B. Kim, R. Theissmann, F. Baier, W.H. Wang, J. Eckert, "Work-hardenable" ductile bulk metallic glass, *Phys. Rev. Lett.* 94 (20) (2005) 205501.
- [16] B. Shi, Y. Xu, C. Li, W. Jia, Z. Li, J. Li, Evolution of free volume and shear band intersections and its effect on hardness of deformed zr_{64.13}cu_{15.75}ni_{10.12}al₁₀ bulk metallic glass, *J. Alloy. Compd.* 669 (2016) 167–176.
- [17] H. Huang, J. Yan, Investigating shear band interaction in metallic glasses by adjacent nanoindentation, *Mater. Sci. Eng.* 704 (2017) 375–385, doi:10.1016/j.msea.2017.08.040.
- [18] C. Liu, A. Das, W. Wang, S. Küchemann, P. Kenesei, R. Maaß, Shear-band cavities and strain hardening in a metallic glass revealed with phase-contrast x-ray tomography, *Scr. Mater.* 170 (2019) 29–33.
- [19] R. Maaß, J.F. Löffler, Shear-band dynamics in metallic glasses, *Adv. Funct. Mater.* 25 (16) (2015) 2353–2368, doi:10.1002/adfm.201404223.
- [20] T.C. Pekin, J. Ding, C. Gammer, B. Ozdol, C. Ophus, M. Asta, R.O. Ritchie, A.M. Minor, Direct measurement of nanostructural change during in situ deformation of a bulk metallic glass, *Nat. Commun.* 10 (1) (2019). 2445–2445
- [21] L.Q. Shen, P. Luo, Y.C. Hu, H.Y. Bai, Y.H. Sun, B.A. Sun, Y.H. Liu, W.H. Wang, Shear-band affected zone revealed by magnetic domains in a ferromagnetic metallic glass, *Nat. Commun.* 9 (1) (2018) 4414.
- [22] D.P. Wang, B.A. Sun, X.R. Niu, Y. Yang, W.H. Wang, C.T. Liu, Mutual interaction of shear bands in metallic glasses, *Intermetallics* 85 (2017) 48–53, doi:10.1016/j.intermet.2017.01.015.
- [23] D.P. Wang, B.A. Sun, M. Gao, Y. Yang, C.T. Liu, The mechanism of shear-band blocking in monolithic metallic glasses, *Mater. Sci. Eng.: A* 703 (2017) 162–166.
- [24] A. Hirata, P.F. Guan, T. Fujita, Y. Hirotsu, A. Inoue, A.R. Yavari, T. Sakurai, M.W. Chen, Direct observation of local atomic order in a metallic glass, *Nat. Mater.* 10 (1) (2011) 28–33.
- [25] D.Z. Chen, C.Y. Shi, Q. An, Q. Zeng, W.L. Mao, W.A. Goddard, J.R. Greer, Fractal atomic-level percolation in metallic glasses, *Science* 349 (6254) (2015) 1306–1310, doi:10.1126/science.aab1233.
- [26] F. Moitzi, D. Şopu, D. Holec, D. Perera, N. Mousseau, J. Eckert, Chemical bonding effects on the brittle-to-ductile transition in metallic glasses, *Acta Mater.* 188 (2020) 273–281.
- [27] Y. Shi, M.L. Falk, Stress-induced structural transformation and shear banding during simulated nanoindentation of a metallic glass, *Acta Mater.* 55 (13) (2007) 4317–4324.
- [28] A. Barbot, M. Lerbinger, A. Hernandez-Garcia, R. Garcia-Garcia, M.L. Falk, D. Vandembroucq, S. Patinet, Local yield stress statistics in model amorphous solids, *Phys. Rev. E* 97 (3) (2018) 033001.
- [29] S. Plimpton, Fast parallel algorithms for short-range molecular-dynamics, *J. Comput. Phys.* 117 (1) (1995) 1–19.
- [30] V. Borovikov, M.I. Mendeleev, A.H. King, Effects of stable and unstable stacking fault energy on dislocation nucleation in nano-crystalline metals, *Modell. Simul. Mater. Sci. Eng.* 24 (8) (2016) 085017.
- [31] M.J. Mees, G. Pourtois, E.C. Neyts, B.J. Thijssse, A. Stesmans, Uniform-acceptance force-bias monte carlo method with time scale to study solid-state diffusion, *Phys. Rev. B* 85 (13) (2012) 134301.

- [32] A. Stukowski, Visualization and analysis of atomistic simulation data with ovito—the open visualization tool, *Modell. Simul. Mater. Sci. Eng.* 18 (1) (2010) 015012.
- [33] G.T. Barkema, N. Mousseau, Event-based relaxation of continuous disordered systems, *Phys. Rev. Lett.* 77 (21) (1996) 4358–4361, doi:10.1103/physrevlett.77.4358.
- [34] R. Malek, N. Mousseau, Dynamics of lennard-jones clusters: a characterization of the activation-relaxation technique, *Phys. Rev. E* 62 (6) (2000) 7723–7728, doi:10.1103/physreve.62.7723.
- [35] N. Mousseau, L.K. Béland, P. Brommer, J.-F. Joly, F. El-Mellouhi, E. Machado-Charry, M. Marinica, P. Pochet, The activation-relaxation technique: art nouveau and kinetic art, *J. Atom. Molecul. Opt. Phys.* 2012 (2012) 1–14, doi:10.1155/2012/925278.
- [36] H.Y. Xu, M.Z. Li, Activation-relaxation technique study on beta-relaxation in La55Ni20Al25 and Cu46Zr46Al8 metallic glasses, *Intermetallics* 94 (2018) 10–16, doi:10.1016/j.intermet.2017.12.017.
- [37] P.M. Piaggi, M. Parrinello, Entropy based fingerprint for local crystalline order, *J. Chem. Phys.* 147 (11) (2017) 114112, doi:10.1063/1.4998408.
- [38] Y. Shi, M.L. Falk, A computational analysis of the deformation mechanisms of a nanocrystalline metallic glass composite, *Acta Mater.* 56 (5) (2008) 995–1000, doi:10.1016/j.actamat.2007.11.005.
- [39] J.C. Lee, K.W. Park, K.H. Kim, E. Fleury, B.J. Lee, M. Wakeda, Y. Shibutani, Origin of the plasticity in bulk amorphous alloys, *J. Mater. Res.* 22 (11) (2007) 3087–3097.
- [40] D.B. Miracle, A structural model for metallic glasses, *Nat. Mater.* 3 (10) (2004) 697–702.
- [41] Y.C. Cheng, E. Ma, Atomic-level structure and structure-property relationship in metallic glasses, *Prog. Mater. Sci.* 56 (4) (2011) 379–473, doi:10.1016/j.pmatsci.2010.12.002.
- [42] Y.S. Wang, G.J. Hao, Y. Zhang, J.P. Lin, L. Song, J.W. Qiao, The role of the interface in a ti-based metallic glass matrix composite with in situ dendrite reinforcement, *Surf. Interface Anal.* 46 (5) (2014) 293–296, doi:10.1002/sia.5413.
- [43] E. Ma, J. Ding, Tailoring structural inhomogeneities in metallic glasses to enable tensile ductility at room temperature, *Mater. Today* 19 (10) (2016) 568–579.
- [44] J.J. Lewandowski, W.H. Wang, A.L. Greer, Intrinsic plasticity or brittleness of metallic glasses, *Phil. Mag. Lett.* 85 (2) (2005) 77–87, doi:10.1080/09500830500080474.
- [45] Y.Q. Cheng, A.J. Cao, E. Ma, Correlation between the elastic modulus and the intrinsic plastic behavior of metallic glasses: the roles of atomic configuration and alloy composition, *Acta Mater.* 57 (11) (2009) 3253–3267.
- [46] J. Ding, Y.-Q. Cheng, H. Sheng, M. Asta, R.O. Ritchie, E. Ma, Universal structural parameter to quantitatively predict metallic glass properties, *Nat. Commun.* 7 (1) (2016) 13733, doi:10.1038/ncomms13733.
- [47] S. Swayamjyoti, J.F. Löffler, P.M. Derlet, Local structural excitations in model glasses, *Phys. Rev. B* 89 (22) (2014) 224201.
- [48] S. Küchemann, R. Maaß, Gamma relaxation in bulk metallic glasses, *Scr. Mater.* 137 (2017) 5–8.
- [49] D. Şopu, A. Stukowski, M. Stoica, S. Scudino, Atomic-level processes of shear band nucleation in metallic glasses, *Phys. Rev. Lett.* 119 (19) (2017) 195503.
- [50] B. Yang, M.L. Morrison, P.K. Liaw, R.A. Buchanan, G. Wang, C.T. Liu, M. Denda, Dynamic evolution of nanoscale shear bands in a bulk-metallic glass, *Appl. Phys. Lett.* 86 (14) (2005) 141904, doi:10.1063/1.1891302.